THE JOURNAL OF PHYSICAL CHEMISTRY A
A JOURNAL OF THE AMERICAN CHEMICAL SOCIETY

pubs.acs.org/JPCA

Article

Electronegativity Force Field for Prediction of Elastic Moduli

Chunbo Zhang and Enlai Gao*

Cite This: J. Phys. Chem. A 2023, 127, 6628−6634

Read Online

ACCESS | Metrics & More | Article Recommendations | Supporting Information

ABSTRACT: Macroscopic elastic moduli (*i.e.*, bulk modulus and shear modulus) of covalent crystals are mainly determined by microscopic structures and stiffnesses. Herein, the microscopic bond and angle force constants of covalent crystals were parameterized from their atomic electronegativities, which is named the electronegativity force field (EFF). Based on this force field, the elastic moduli of covalent crystals can be directly obtained by molecular mechanics calculations. The calculated moduli for various covalent crystals are generally consistent with first-principles calculations, while the computational cost is reduced by several orders of magnitude, indicating the accuracy and efficiency of the EFF. Finally, we found 25 ultrahigh-modulus crystals with a bulk modulus greater than 350 GPa, which demonstrates that this force field can be used for screening of ultrahigh-modulus materials from numerous crystal candidates.

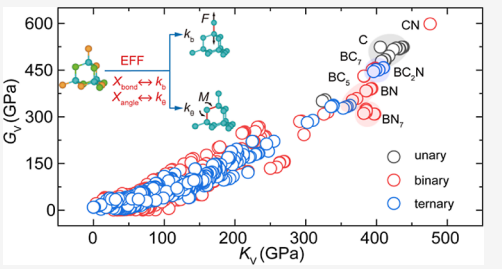

INTRODUCTION

Elastic moduli (*i.e.*, bulk modulus and shear modulus) not only measure the resistance to elastic deformation but are also closely related to other important properties of a material. For example, the bulk modulus has been used as an indication to screen superhard materials since a high bulk modulus is generally essential for superhard crystals.[1] High-modulus materials have been used in a wide range of scientific and industrial applications[2−4] from high-pressure science to precision machining.

Driven by the increasing demand for high-modulus materials, several approaches have been developed to determine the elastic moduli of materials, including experimental measurements,[5] first-principles calculations,[6−8] classical molecular dynamics simulations,[9−11] empirical/semi-empirical formulae,[12−18] and machine learning prediction.[19] Using these approaches, remarkable achievements have been made, and a few high-modulus materials with a bulk modulus rivaling or exceeding that of diamond, such as C_3N_4 (425−496 GPa),[7] BN (400 GPa),[20,21] ReC (422 GPa),[22] and lonsdaleite (437 GPa),[23,24] have been reported. However, as the number of crystal structures identified from experiments and computations in material databases [*e.g.*, the Crystallography Open Database (COD),[25] Inorganic Crystal Structure Database (ICSD),[26] Materials Project (MP),[27] and Open Quantum Materials Database (OQMD)[28]] grows rapidly, it becomes challenging to determine elastic moduli using the above-mentioned approaches. This is because classical molecular dynamics and empirical/semi-empirical formulae are only applicable for specific elemental combinations with limited accuracy, while experimental measurements and first-principles calculations are too expensive and time-consuming. For example, after decades of calculations, only about 10^4 crystals in the Materials Project[27] (on the order of 1% of all known crystal structures, as shown in Table S1) have first-principles-calculated elastic constants. Hence, approaches for determining the elastic moduli of materials that can balance accuracy and efficiency are needed.

Macroscopic elastic moduli of covalent crystals are mainly determined by microscopic bond and angle stiffnesses[29,30] that essentially originate from elemental combinations. Hence, it is possible to estimate the elastic moduli of a material solely from its elemental combinations. As pioneers, Rappe *et al.*[31] developed a universal force field (UFF) in which the force field parameters for the full periodic table of elements are estimated using general rules based only on the element, its hybridization, and its connectivity. However, the calculated moduli using the UFF are far from first-principles calculations, as demonstrated in our following investigation. Li and Xue proposed electronegativity scales for ionic[32] and covalent[33] crystals, which have been used in empirical formulae for predicting the bulk modulus[15] and hardness[14,33] for specific covalent crystals. The usefulness of these formulae indicates the feasibility of predicting macroscopic properties from elemental combinations.

In the present work, we developed an electronegativity force field (EFF) in which the bond and angle force constants of covalent crystals were determined from the atomic electronegativities. The calculated bulk and shear moduli of unary, binary, and ternary covalent crystals using this force field are well consistent with those of first-principles calculations, while

Received: May 14, 2023
Revised: June 26, 2023
Published: July 31, 2023

https://doi.org/10.1021/acs.jpca.3c03173
J. Phys. Chem. A 2023, 127, 6628−6634

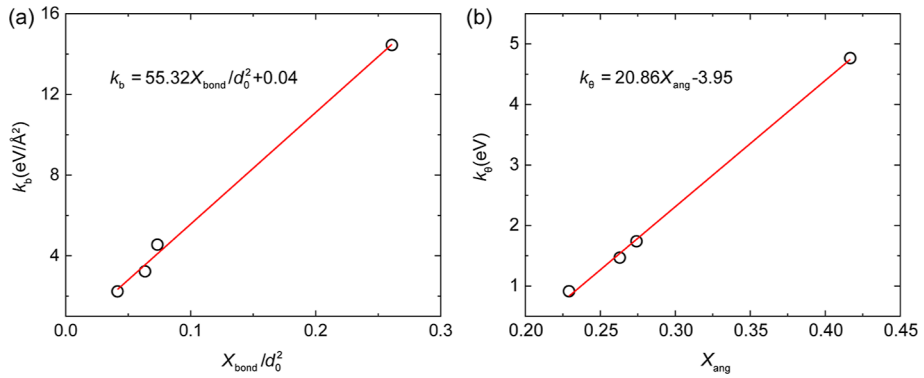

Figure 1. (a) Relationship between k_b and $X_{bond}/{d_0}^2$ and (b) relationship between k_θ and X_{ang} for nonpolar covalent crystals.

the computational cost is reduced by several orders of magnitude. These results demonstrate the accuracy and efficiency of the EFF. Finally, the EFF was used for screening ultrahigh-modulus materials from known crystal structures, which accelerated the discovery of 25 ultrahigh-modulus crystals with a bulk modulus greater than 350 GPa.

METHODS

The present goal is to predict the bulk and shear moduli of covalent crystals from their elemental combinations. Considering that the macroscopic bulk and shear moduli of covalent crystals are mainly from the contribution of bond stretching and angle bending, we first established formulae between bond and angle force constants and atomic electronegativities, named the EFF. By using the EFF, the elastic constants of covalent crystals can be calculated by using molecular mechanics methods. From the calculated elastic constants, the bulk and shear moduli can be extracted.

In addition to bond stretching and angle bending, we also explored the effects of dihedral and vdW interactions. Our calculations show that the differences between bulk and shear moduli of diamond with and without considering dihedral and vdW interactions are less than 10%. These results indicate that the macroscopic strain energy is mainly contributed by microscopic energies of bond stretching and angle bending, which can be described by $V_b = k_b(d - d_0)^2$ and $V_a = k_\theta(\theta - \theta_0)^2$, respectively, where the parameters of d_0, θ_0, k_b, and k_θ are the equilibrium bond length, equilibrium angle, bond force constant, and angle force constant, respectively. Since d_0 and θ_0 can be obtained from the known crystal structure, we only need to determine k_b and k_θ in the following investigation. Electronegativity is an important parameter that scales the holding energy between atoms and valence electrons. The bond electronegativity is a measure of the resistance to the bond stretching,[14] which can be defined as

$$X_{bond} = \sqrt{\frac{X_a \times X_b}{N_a \times N_b}} \tag{1}$$

for a bond formed between atoms a and b, where X_a (N_a) and X_b (N_b) are the electronegativities[33] (connected bond numbers or coordination number) of atoms a and b, respectively. Similarly, the angle electronegativity is a measure of the resistance to the angle bending, which can be defined as

$$X_{ang} = \sqrt[3]{\frac{X_a \times X_b \times X_c}{N_{aa} \times N_{ab} \times N_{ac}}} \tag{2}$$

for an angle formed among atoms a, b, and c, where X_a (N_{aa}), X_b (N_{ab}), and X_c (N_{ac}) are the electronegativities (connected angle numbers) of atoms a, b, and c, respectively. For nonpolar covalent crystals, we found that k_b and k_θ are linear to $X_{bond}/{d_0}^2$ and X_{ang}, respectively (Figure 1). By fitting the known data for four typical nonpolar covalent crystals [C, Si, Ge, and Sn (α-Sn)], the formulae for the prediction of the bond and angle force constants from the electronegativities can be written as

$$k_b = \frac{55.32X_{bond}}{d_0^2} + 0.04 \tag{3}$$

$$k_\theta = 20.86X_{ang} - 3.95 \tag{4}$$

where the units of k_b, d_0, and k_θ are eV/Å^2, Å, and eV, respectively. It should be noted that the existing accurate force fields are usually limited to a narrow range of elements, such as B, C, N, and O. Our work provides a fast and universal approach to determine the force constants from the atomic electronegativities. Meanwhile, taking diamond as an example, we compared our force field with other well-known force fields in the literature[31,34−36] (Table S2). These results indicate that our force field is generally more accurate than previous force fields when comparing with density functional theory (DFT) calculations.

It should be noted that eqs 3 and 4 were developed for nonpolar covalent crystals (C, Si, Ge, and α-Sn). For polar covalent crystals, the difference of the electronegativities of atoms in chemical bonds and angles will destroy the uniform distribution of valence electrons, which will weaken the resistances to the bond stretching and the angle bending. As a result, the ionicity of polar covalent crystals would reduce the bond and angle force constants because of the asymmetry distribution of valence electrons in chemical bonds and angles. Hence, the predicted moduli for polar covalent crystals using the above formulae (eqs 3 and 4) are generally overestimated compared with those from first-principles calculations (Figure S1). To address this issue, we proposed the bond ionicity (f_b) and angle ionicity (f_a) to take the ionicity-induced reduction of force constants into account.

$$f_b = \frac{|X_a - X_b|}{X_a + X_b} \tag{5}$$

$$f_a = \frac{|X_a - X_b|}{X_a + X_b} + \frac{|X_a - X_c|}{X_a + X_c} \tag{6}$$

From the bond ionicity and angle ionicity, eqs 3 and 4 were modified by introducing the exponential loss functions of ${f_b}^2$

https://doi.org/10.1021/acs.jpca.3c03173
J. Phys. Chem. A 2023, 127, 6628−6634

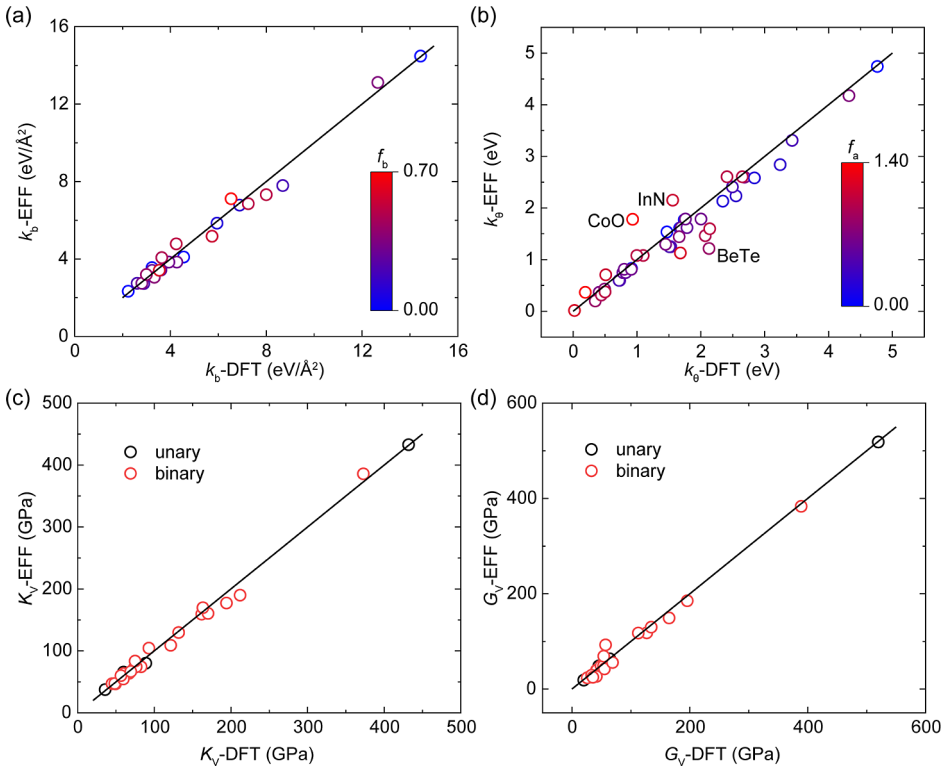

Figure 2. (a) Bond force constants and (b) angle force constants for covalent crystals from eqs 7 and 8 as compared with those from first-principles calculations. (c) Bulk moduli and (d) shear moduli for covalent crystals calculated based on the EFF as compared with first-principles calculations. The raw training data set is summarized in Table S3.

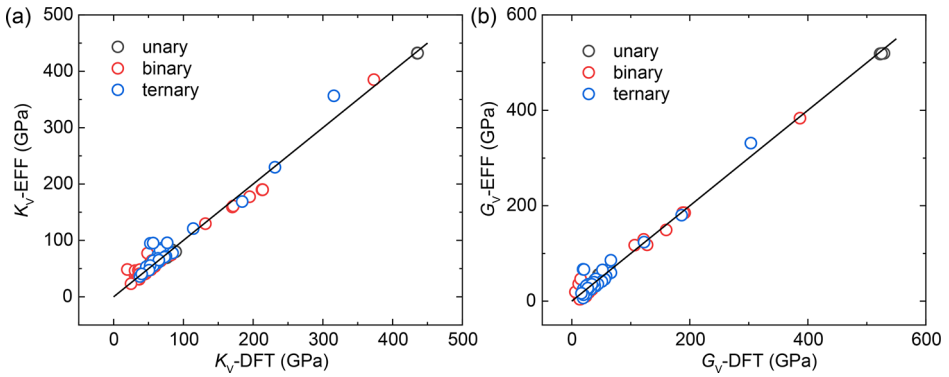

Figure 3. (a) Predicted bulk moduli and (b) shear moduli based on the EFF as compared with corresponding first-principles-calculated moduli. The test data set is not overlapped with the previous training data set in Figure 2.

and f_a^2. Similar exponential loss functions have also been adopted to predict the mechanical properties of covalent crystals in previous works.[14,15] By fitting the data for 25 unary and binary crystals from DFT calculations (see Supporting Information for this training data set), the fitting formulae for predicting the bond and angle force constants of polar covalent crystals were generalized as

$$k_b = \left(\frac{55.32X_{bond}}{d_0^2} + 0.04\right)e^{-0.16f_b^2} \quad (7)$$

$$k_\theta = (20.86X_{ang} - 3.95)e^{-0.51f_a^2} \quad (8)$$

Here, d_0 is adopted as the equilibrium bond length in the crystal. For these unary and binary crystals, there is only one type of bond. As shown in Figure 2, the force constants and elastic moduli for polar covalent crystals predicted by these generalized formulae are consistent with first-principles calculations. To further quantify the accuracy of the fitting results with respect to first-principles calculations, the mean error (ME), mean absolute error (MAE), mean relative error (MRE), and mean absolute relative error (MARE) were calculated. The calculated ME, MAE, MRE, and MARE for the bulk (shear) modulus based on the EFF are −1.81 (−2.92) GPa, 6.32 (7.57) GPa, −1.05 (−5.02)%, and 5.99 (13.06)%, respectively. These results indicate that the fitting results of the EFF are in good agreement with those of first-principles calculations.

RESULTS AND DISCUSSION

Based on the atomic electronegativities, eqs 7 and 8 can be used to predict the force constants of covalent crystals. Based

https://doi.org/10.1021/acs.jpca.3c03173
J. Phys. Chem. A 2023, 127, 6628−6634

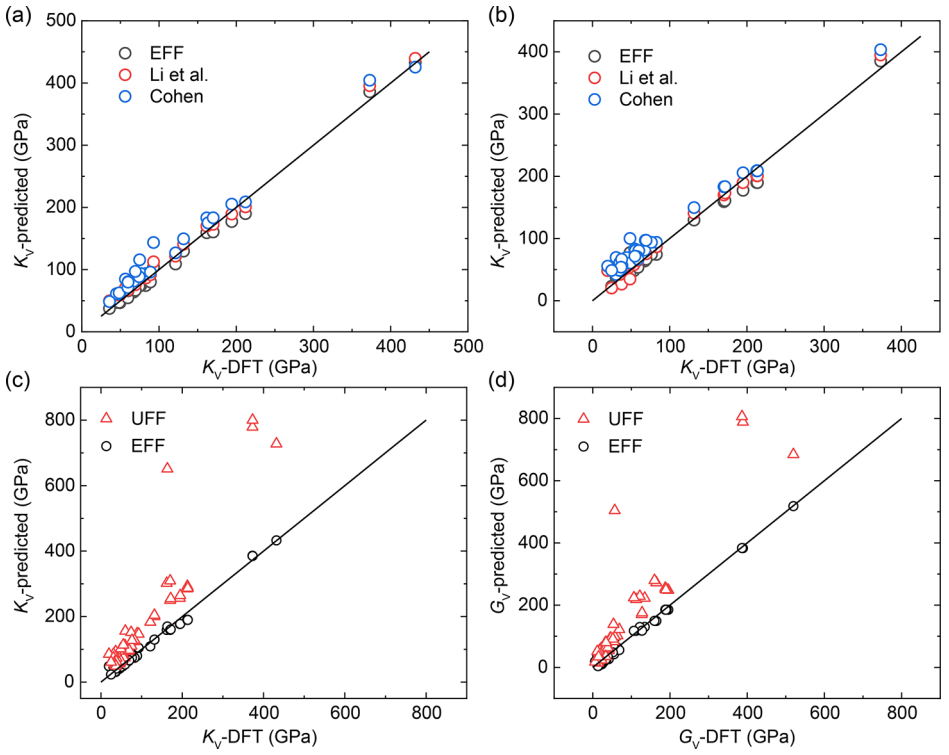

Figure 4. (a) Predicted bulk moduli of 25 crystals from the Materials Project based on the EFF, Li *et al.*,[15] and Cohen[13] as compared with those from first-principles calculations. (b) Predicted bulk moduli of 63 binary covalent crystals from the Materials Project based on the EFF, Li *et al.*,[15] and Cohen[13] as compared with those from first-principles calculations. (c) Bulk and (d) shear moduli of 88 covalent crystals predicted based on the EFF and the UFF as compared with first-principles calculations.

on the EFF, the elastic constants of known crystal structures can be determined by molecular mechanics calculations. These calculations were performed using the large-scale atomic/molecular massively parallel simulator (LAMMPS),[37] in which the elastic constants are calculated by strain−stress methods.[38]

To validate the accuracy of the prediction based on the EFF, we did tests on 110 covalent crystals (test data set that is not overlapped with the previous training data set), including 13 unary crystals, 63 binary crystals, and 34 ternary crystals. From the EFF-predicted force constants and crystal structures, the elastic moduli were calculated by molecular mechanics calculations (Figure 3 and Tables S4−S6). In general, the predicted moduli based on the EFF are in good agreement with those based on first-principles calculations. More specifically, the EFF model has demonstrated accurate predictions for tetrahedral covalent crystals with a Pauling electronegativity difference between the two atoms of less than 1.7[39] (Figure S3). To further quantify the accuracy, we calculated the ME, MAE, MRE, and MARE for the predicted bulk (shear) moduli based on the EFF with respect to first-principles calculations as −1.79 (−1.16) GPa, 8.85 (7.58) GPa, 2.57 (0.54)%, and 11.27 (28.28)%, respectively (Table S7). Considering that the deviations of elastic moduli between first-principles calculations from different functionals are about 10−20%,[40] these results indicate that the accuracy of the prediction based on the EFF falls within the range of intrinsic errors of first-principles calculations. Hence, the accuracy of the prediction based on the EFF is comparable to that of first-principles calculations. We also compared the predicted bulk moduli based on the EFF with those based on empirical/semi-empirical formulae for estimation of the bulk moduli proposed by Cohen[13] and Li *et al.*[15] (Figure 4a,b). The calculated ME, MAE, MRE, and MARE with respect to first-principles calculations (Table 1) indicate that the accuracy of the prediction based on the EFF is improved compared with those of Li et al.[15] and Cohen.[13] In addition to comparisons with empirical/semi-empirical formulae, we also compared the predicted moduli based on the EFF with those based on the widely used UFF.[31] As shown in Figure 4c,d, the elastic moduli are generally overestimated by the UFF. The calculated ME, MAE, MRE, and MARE of the UFF with respect to first-principles calculations are all much higher than those of the EFF (Table S8). These results indicate that the accuracy of the

Table 1. ME, MAE, MRE, and MARE of Bulk Moduli Predicted by the EFF, Li *et al.*,[15] and Cohen[13] with Respect to First-Principles Calculations[a]

	EFF	Li *et al*	Cohen
	25 fitting crystals		
ME (GPa)	−1.81	9.27	16.74
MAE (GPa)	6.32	10.56	17.51
MRE (%)	−1.05	13.20	21.96
MARE (%)	5.99	13.82	22.20
	63 binary crystals		
ME (GPa)	−5.53	3.46	14.85
MAE (GPa)	10.03	10.52	16.96
MRE (%)	0.44	13.50	32.66
MARE (%)	12.36	18.80	33.65

[a]Note: 25 crystals in the training data set were used for comparison in this table. Unless otherwise noted, the elastic moduli were obtained from the Materials Project.

https://doi.org/10.1021/acs.jpca.3c03173
J. Phys. Chem. A 2023, 127, 6628−6634

prediction based on the EFF is significantly improved compared with previous works.

The efficiency of the EFF was also explored by comparing the computational time for 25 crystals in the training data set (Figure S2). The average duration for calculating the elastic tensor of a crystal is less than 1 s with a single central processing unit, and the ratio of computational duration between first-principles calculations and calculations based on the EFF is as high as 3×10^5. These results indicate that the computational cost of the EFF is largely reduced by over 5 orders of magnitude compared with that of first-principles calculations. To summarize, the predicted elastic moduli from the EFF are comparable to those from first-principles calculations, while the computational cost is neglectable, indicating the accuracy and efficiency of the EFF. Such accuracy and efficiency make the EFF hold great promise for screening ultrahigh-modulus materials from numerous crystal candidates.

Finally, we employed the EFF to discover high-modulus materials by prescreening numerous crystal candidates in the Materials Project (MP)[27] and the Open Quantum Materials Database (OQMD).[28] First, a total of 3139 tetrahedral crystals in the MP (870 crystals) and OQMD (2269 crystals) were selected. Afterward, molecular mechanics calculations based on the EFF were employed to predict the bulk and shear moduli of these crystals (Figure 5). From these predictions, we found

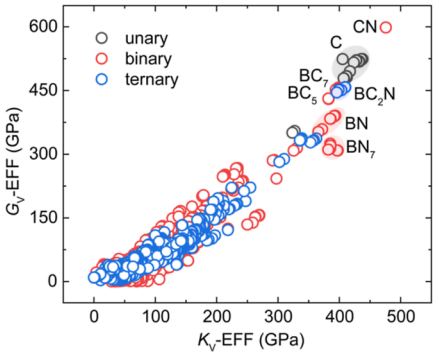

Figure 5. Predicted elastic moduli for 3139 crystal candidates in the Materials Project (MP)[27] and the Open Quantum Materials Database (OQMD).[28]

39 unique crystals with a predicted bulk modulus over 300 GPa. The highest bulk modulus (475.7 GPa) and shear modulus (598.5 GPa) belonged to CN (OQMD-1218937). However, the first-principles calculations show that the elastic tensor of this crystal is not positive definite, indicating its mechanical instability. Finally, first-principles verification identified that 25 ultrahigh-modulus crystals meet the Born stability criteria[41] and have a bulk modulus greater than 350 GPa (Table S9). The highest energy above hull for these crystals is 0.83 eV/atom, which is lower than the metastability threshold[42] (Table S9). This implies that these 25 crystals are all promising for fabrication. We found that most high-modulus crystals are sp^3 carbon crystals and compounds of BN and BC. These results suggest that light elements B, C, and N with large values of electronegativity are good candidates to form high-modulus crystals.[43] Additionally, the above results indicate that the EFF performs well in predicting the bulk and shear moduli for covalent crystals. From the bulk and shear moduli, the hardness of a crystal can be estimated[44]

$$H_V = \frac{0.55K_{VRH}G_{VRH}}{3K_{VRH} + G_{VRH}} \quad (9)$$

where the K_{VRH} and G_{VRH} are the Hill-averaged[45] bulk modulus and shear modulus, respectively. We calculated the hardness for 135 tetrahedral crystals and compared them with first-principles calculation results (Figure 6). It can be found

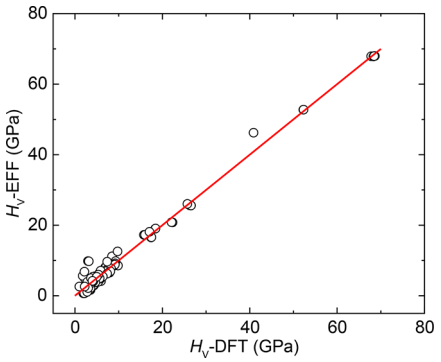

Figure 6. Predicted hardness for 135 crystals based on the EFF as compared with first-principles calculations.

that the hardness predicted by the EFF is also consistent with that predicted by first-principles calculations. This indicates that the EFF has a good performance in predicting the hardness of crystals.

CONCLUSIONS

In summary, we proposed an EFF to calculate the elastic moduli of covalent crystals in which the bond and angle force constants of covalent crystals were determined from the atomic electronegativities. Based on this force field, the elastic moduli of covalent crystals can be directly obtained by molecular mechanics calculations. The predicted bulk and shear moduli of unary, binary, and ternary covalent crystals using this force field from the EFF are comparable to those of first-principles calculations, while the computational cost is neglectable, indicating the accuracy and efficiency of the EFF. Finally, we used the EFF to screen ultrahigh-modulus materials from numerous crystal candidates and identified 25 ultrahigh-modulus crystals with a bulk modulus greater than 350 GPa. Additionally, the promising use of the EEF for predicting the hardness of crystals was discussed.

ASSOCIATED CONTENT

Supporting Information

The Supporting Information is available free of charge at https://pubs.acs.org/doi/10.1021/acs.jpca.3c03173.

Methods to parameterize the EFF and application of the EFF, and supplmentary figures and tables (PDF)

AUTHOR INFORMATION

Corresponding Author

Enlai Gao − *Department of Engineering Mechanics, School of Civil Engineering, Wuhan University, Wuhan, Hubei 430072, China;* orcid.org/0000-0003-1960-0260; Email: enlaigao@whu.edu.cn

https://doi.org/10.1021/acs.jpca.3c03173
J. Phys. Chem. A 2023, 127, 6628−6634

Author

Chunbo Zhang − *Department of Engineering Mechanics, School of Civil Engineering, Wuhan University, Wuhan, Hubei 430072, China*

Complete contact information is available at: https://pubs.acs.org/10.1021/acs.jpca.3c03173

Notes

The authors declare no competing financial interest.

■ ACKNOWLEDGMENTS

This work in China was supported by the National Natural Science Foundation of China (12172261). The numerical calculations in this work were done on the supercomputing system in the Supercomputing Center of Wuhan University.

■ REFERENCES

(1) Haines, J.; Léger, J. M.; Bocquillon, G. Synthesis and Design of Superhard Materials. *Annu. Rev. Mater. Res.* **2001**, *31*, 1−23.

(2) Anderson, O. L.; Nafe, J. E. The Bulk Modulus-Volume Relationship for Oxide Compounds and Related Geophysical Problems. *J. Geophys. Res.* **1965**, *70*, 3951−3963.

(3) Laio, A.; Bernard, S.; Chiarotti, G. L.; Scandolo, S.; Tosatti, E. Physics of Iron at Earth's Core Conditions. *Science* **2000**, *287*, 1027−1030.

(4) Steinle-Neumann, G.; Stixrude, L.; Cohen, R. E.; Gulseren, O. Elasticity of Iron at the Temperature of the Earth's Inner Core. *Nature* **2001**, *413*, 57−60.

(5) Mattesini, M.; de Almeida, J. S.; Dubrovinsky, L.; Dubrovinskaia, N.; Johansson, B.; Ahuja, R. High-Pressure and High-Temperature Synthesis of the Cubic TiO_2 Polymorph. *Phys. Rev. B* **2004**, *70*, 212101.

(6) Swamy, V.; Muddle, B. C. Ultrastiff Cubic TiO_2 Identified Via First-Principles Calculations. *Phys. Rev. Lett.* **2007**, *98*, 035502.

(7) Teter, D. M.; Hemley, R. J. Low-Compressibility Carbon Nitrides. *Science* **1996**, *271*, 53−55.

(8) Peng, B.; Mortazavi, B.; Zhang, H.; Shao, H.; Xu, K.; Li, J.; Ni, G.; Rabczuk, T.; Zhu, H. Tuning Thermal Transport in C_3N Monolayers by Adding and Removing Carbon Atoms. *Phys. Rev. Appl.* **2018**, *10*, 034046.

(9) Gao, G.; Workum, K. V.; Schall, J. D.; Harrison, J. A. Elastic Constants of Diamond from Molecular Dynamics Simulations. *J. Phys. Condens. Matter* **2006**, *18*, S1737−S1750.

(10) Gao, F.; Qu, J. Calculating the Diffusivity of Cu and Sn in Cu_3Sn Intermetallic by Molecular Dynamics Simulations. *Mater. Lett.* **2012**, *73*, 92−94.

(11) Favaro, G.; Bazzan, M.; Amato, A.; Arciprete, F.; Cesarini, E.; Corso, A. J.; De Matteis, F.; Dao, T. H.; Granata, M.; Honrado-Benítez, C.; et al. Measurement and Simulation of Mechanical and Optical Properties of Sputtered Amorphous SiC Coatings. *Phys. Rev. Appl.* **2022**, *18*, 044030.

(12) Harrison, W. A. *Instructor's Guide and Solutions Manual for Electronic Structure and the Properties of Solids: The Physics of the Chemical Bond*; W. H. Freeman, 1980.

(13) Cohen, M. L. Calculation of Bulk Moduli of Diamond and Zinc-Blende Solids. *Phys. Rev. B* **1985**, *32*, 7988−7991.

(14) Li, K.; Wang, X.; Zhang, F.; Xue, D. Electronegativity Identification of Novel Superhard Materials. *Phys. Rev. Lett.* **2008**, *100*, 235504.

(15) Li, K.; Ding, Z.; Xue, D. Electronegativity-Related Bulk Moduli of Crystal Materials. *Phys. Status Solidi B* **2011**, *248*, 1227−1236.

(16) Mattsson, A. E.; Schultz, P. A.; Desjarlais, M. P.; Mattsson, T. R.; Leung, K. Designing Meaningful Density Functional Theory Calculations in Materials Science—A Primer. *Modell. Simul. Mater. Sci. Eng.* **2004**, *13*, R1−R31.

(17) Ravindran, P.; Fast, L.; Korzhavyi, P. A.; Johansson, B.; Wills, J.; Eriksson, O. Density Functional Theory for Calculation of Elastic Properties of Orthorhombic Crystals: Application to $TiSi_2$. *J. Appl. Phys.* **1998**, *84*, 4891−4904.

(18) Kamran, S.; Chen, K.; Chen, L. Semiempirical Formulae for Elastic Moduli and Brittleness of Diamondlike and Zinc-Blende Covalent Crystals. *Phys. Rev. B* **2008**, *77*, 094109.

(19) Shao, Q.; Li, R.; Yue, Z.; Wang, Y.; Gao, E. Data-Driven Discovery and Understanding of Ultrahigh-Modulus Crystals. *Chem. Mater.* **2021**, *33*, 1276−1284.

(20) Deura, M.; Kutsukake, K.; Ohno, Y.; Yonenaga, I.; Taniguchi, T. Nanoindentation Measurements of a Highly Oriented Wurtzite-Type Boron Nitride Bulk Crystal. *Jpn. J. Appl. Phys.* **2017**, *56*, 030301.

(21) Zhou, R.; Dai, J.; Cheng Zeng, X. Structural, Electronic and Mechanical Properties of sp^3-Hybridized BN Phases. *Phys. Chem. Chem. Phys.* **2017**, *19*, 9923−9933.

(22) Chen, Z.; Gu, M.; Sun, C. Q.; Zhang, X.; Liu, R. Ultrastiff Carbides Uncovered in First Principles. *Appl. Phys. Lett.* **2007**, *91*, 061905.

(23) Qingkun, L.; Yi, S.; Zhiyuan, L.; Yu, Z. Lonsdaleite − A Material Stronger and Stiffer Than Diamond. *Scr. Mater.* **2011**, *65*, 229−232.

(24) Kulnitskiy, B.; Perezhogin, I.; Dubitsky, G.; Blank, V. Polytypes and Twins in the Diamond−Lonsdaleite System Formed by High-Pressure and High-Temperature Treatment of Graphite. *Acta Crystallogr., Sect. B: Struct. Sci., Cryst. Eng. Mater.* **2013**, *69*, 474−479.

(25) Grazulis, S.; Chateigner, D.; Downs, R. T.; Yokochi, A. F.; Quiros, M.; Lutterotti, L.; Manakova, E.; Butkus, J.; Moeck, P.; Le Bail, A. Crystallography Open Database - An Open-Access Collection of Crystal Structures. *J. Appl. Crystallogr.* **2009**, *42*, 726−729.

(26) Zagorac, D.; Müller, H.; Ruehl, S.; Zagorac, J.; Rehme, S. Recent Developments in the Inorganic Crystal Structure Database: Theoretical Crystal Structure Data and Related Features. *J. Appl. Crystallogr.* **2019**, *52*, 918−925.

(27) Jain, A.; Ong, S. P.; Hautier, G.; Chen, W.; Richards, W. D.; Dacek, S.; Cholia, S.; Gunter, D.; Skinner, D.; Ceder, G.; et al. Commentary: The Materials Project: A Materials Genome Approach to Accelerating Materials Innovation. *APL Mater.* **2013**, *1*, 011002.

(28) Saal, J. E.; Kirklin, S.; Aykol, M.; Meredig, B.; Wolverton, C. Materials Design and Discovery with High-Throughput Density Functional Theory: The Open Quantum Materials Database (OQMD). *J. Met., Mater. Miner.* **2013**, *65*, 1501−1509.

(29) Liu, A. Y.; Cohen, M. L. Prediction of New Low Compressibility Solids. *Science* **1989**, *245*, 841−842.

(30) Tanaka, K.; Okamoto, K.; Inui, H.; Minonishi, Y.; Yamaguchi, M.; Koiwa, M. Elastic Constants and Their Temperature Dependence for the Intermetallic Compound Ti_3Al. *Philos. Mag. A* **1996**, *73*, 1475−1488.

(31) Rappe, A. K.; Casewit, C. J.; Colwell, K. S.; Goddard, W. A.; Skiff, W. M. UFF, A Full Periodic Table Force Field for Molecular Mechanics and Molecular Dynamics Simulations. *J. Am. Chem. Soc.* **2002**, *114*, 10024−10035.

(32) Li, K.; Xue, D. Estimation of Electronegativity Values of Elements in Different Valence States. *J. Phys. Chem. A* **2006**, *110*, 11332−11337.

(33) Li, K.; Wang, X.; Xue, D. Electronegativities of Elements in Covalent Crystals. *J. Phys. Chem. A* **2008**, *112*, 7894−7897.

(34) Boyd, P. G.; Moosavi, S. M.; Witman, M.; Smit, B. Force-Field Prediction of Materials Properties in Metal-Organic Frameworks. *J. Phys. Chem. Lett.* **2017**, *8*, 357−363.

(35) Hagler, A. T.; Lifson, S.; Dauber, P. Consistent Force Field Studies of Intermolecular Forces in Hydrogen-Bonded Crystals. 2. A Benchmark for the Objective Comparison of Alternative Force Fields. *J. Am. Chem. Soc.* **2002**, *101*, 5122−5130.

(36) Sun, H.; Mumby, S. J.; Maple, J. R.; Hagler, A. T. An *ab* Initio CFF93 All-Atom Force Field for Polycarbonates. *J. Am. Chem. Soc.* **2002**, *116*, 2978−2987.

(37) Thompson, A. P.; Aktulga, H. M.; Berger, R.; Bolintineanu, D. S.; Brown, W. M.; Crozier, P. S.; in't Veld, P. J.; Kohlmeyer, A.; Moore, S. G.; Nguyen, T. D.; et al. Lammps - A Flexible Simulation

Tool for Particle-Based Materials Modeling at the Atomic, Meso, and Continuum Scales. *Comput. Phys. Commun.* **2022**, *271*, 108171.
(38) Rassoulinejad-Mousavi, S. M.; Mao, Y.; Zhang, Y. Evaluation of Copper, Aluminum, and Nickel Interatomic Potentials on Predicting the Elastic Properties. *J. Appl. Phys.* **2016**, *119*, 244304.
(39) Pauling, L. *The Nature of the Chemical Bond*; 3rd Ed.; Cornell University: Ithaca, 1960.
(40) Ahmad, Z.; Viswanathan, V. Quantification of Uncertainty in First-Principles Predicted Mechanical Properties of Solids: Application to Solid Ion Conductors. *Phys. Rev. B* **2016**, *94*, 064105.
(41) Born, M.; Huang, K. *Dynamical Theory of Crystal Lattices*; Clarendon Press, 1954.
(42) Aykol, M.; Dwaraknath, S. S.; Sun, W.; Persson, K. A. Thermodynamic Limit for Synthesis of Metastable Inorganic Materials. *Sci. Adv.* **2018**, *4*, No. eaaq0148.
(43) Kurakevych, O. O. Superhard Phases of Simple Substances and Binary Compounds of the B-C-N-O System: From Diamond to the Latest Results (A Review). *J. Superhard Mater.* **2009**, *31*, 139−157.
(44) Ivanovskii, A. L. Hardness of Hexagonal AlB_2-Like Diborides of *s, p* and *d* Metals from Semi-Empirical Estimations. *Int. J. Refract. Met. Hard Mater.* **2013**, *36*, 179−182.
(45) Hill, R. The Elastic Behaviour of a Crystalline Aggregate. *Proc. Phys. Soc., London, Sect. A* **1952**, *65*, 349−354.

https://doi.org/10.1021/acs.jpca.3c03173
J. Phys. Chem. A 2023, 127, 6628−6634

Supporting Information for

Electronegativity Force Field for Prediction of Elastic Moduli

Chunbo Zhang and Enlai Gao*

Department of Engineering Mechanics, School of Civil Engineering, Wuhan University, Wuhan, Hubei 430072, China.

*Corresponding author. Email: enlaigao@whu.edu.cn

This supporting information contains:

(1) Methods to Parameterize the Electronegativity Force Field.

(2) Application of the Electronegativity Force Field.

(3) Figures S1-S3.

(4) Tables S1-S9.

Methods to Parameterize the Electronegativity Force Field.

To show how to get the EFF model, we took the bond stiffness and angle stiffness of unary tetrahedral crystals of C, Si, Ge, and α-Sn as an example. First, we calculated elastic constants of C, Si, Ge, and α-Sn by first-principles calculations. The first-principles density functional theory (DFT) calculations were performed with the Vienna *Ab-Initio* Simulation Package (VASP).[1] The Perdew-Burke-Ernzerhof parameterization of the generalized gradient approximation was used for the exchange-correlation functional.[2] An energy cut-off of 520 eV was employed. A *k*-point mesh with a density about 40 Å (the product of each lattice constant and the corresponding number of *k*-points) was used in Brillouin zone sampling.[3] The conjugate gradient algorithm was adopted for structural relaxation. The energy and the forces were converged to 1×10^{-8} eV/atom and 1×10^{-2} eV/Å, respectively. For these four unary covalent crystals, there is only one type of bond and angle. The bond and angle stiffnesses were obtained by fitting the first-principles calculated bulk and shear moduli[4] converged to the absolute error of less than 1 GPa. Then, we took the bond stiffness and angle stiffnesses of crystal BN as an example. For the BN crystal, there are one type of bond and two types of angles. Therefore, we have one bond stiffness and two angle stiffnesses. The assumption was that the ratio of two angle stiffness equals the angle stiffness obtained from **eq 4**. By substituting the electronegativity[5] and angle electronegativity into **eqs 2** and **4**, we obtained the ratio of angle stiffness of angle ∠BNB (3.350 eV) and ∠NBN (5.389 eV) as 1.609. Then, we changed the angle stiffness of ∠BNB, while the angle stiffness of ∠NBN was calculated by the product of the angle stiffness ∠BNB and angle stiffness ratio 1.609. Finally, we obtained the bond and angle stiffness as 12.659 eV/Å^2, 2.685 eV(∠BNB), and 4.320 eV(∠NBN), respectively.

Application of the Electronegativity Force Field.

To show how to use EFF model for obtaining the parameters of bond and angle stiffness, we took binary tetrahedral crystal BN as an example. In the BN crystal, there are 8 atoms in the conventional cell, 4 B atoms tetrahedrally bonded with N atoms. The bond electronegativity (X_{bond}) and bond ionicity (f_b) can be obtained by substituting the atom electronegativity[5] into **eqs 1** and **5** as 0.594 and 0.354 respectively. From BN crystal structure, we can obtain the bond length (d_0) of BN, which is 1.570 Å. Then, the bond stiffness k_b for harmonic bond of B-N was obtained as 13.098 eV/Å^2 from **eq 7**.

There are two types of angles and 48 angles in the conventional cell, the ratio of angle numbers for ∠BNB and ∠NBN are 1/2 and 1/2, respectively. The angle electronegativity and angle ionicity of ∠BNB (∠NBN) can be obtained by substituting the atom electronegativity[5] into **eqs 2** and **6** as 0.350 (0.448) and 0.707 (0.707), respectively. By substituting the angle electronegativity and angle ionicity (f_a) into **eq 8**, we obtained the harmonic angle stiffness k_θ of ∠BNB and ∠NBN as 2.595 eV and 4.176 eV, respectively. It should be noted that crystal structures were obtained from the database, and the elastic constants were obtained from molecular mechanics with LAMMPS.[6] Then, the EFF predicted bulk modulus (K_V-EFF) and shear modulus (G_V-EFF) were obtained from elastic constants as 385.8 GPa and 383.2 GPa, respectively, which are close to the DFT results (372.9 GPa and 389.0 GPa).

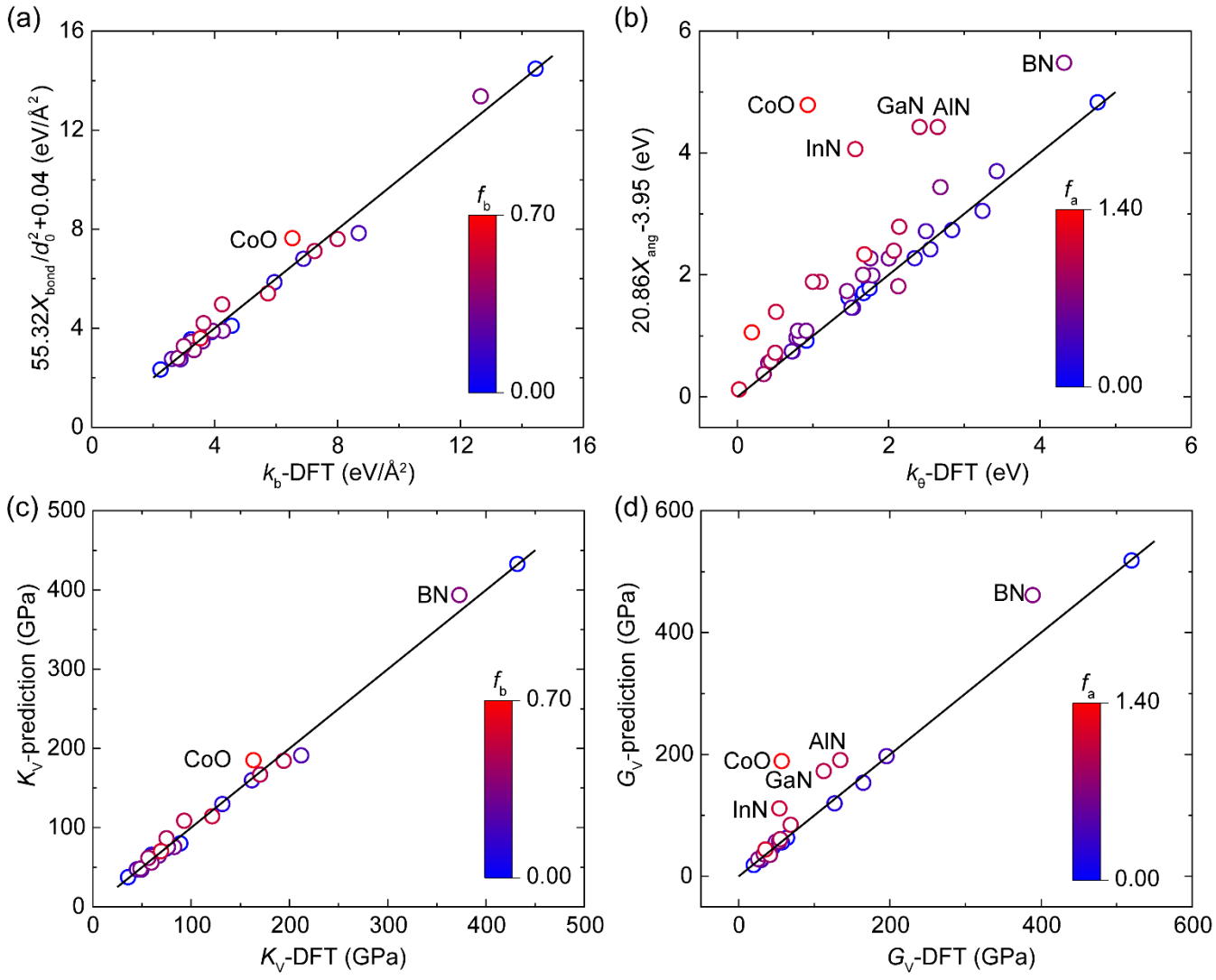

Figure S1. Predicted (a) bond force constants and (b) angle force constants for covalent crystals from **eqs 3** and **4** as compared with first-principles calculations. (c) Bulk moduli and (d) shear moduli for covalent crystals calculated based on the **eqs 3** and **4** as compared with first-principles calculations.

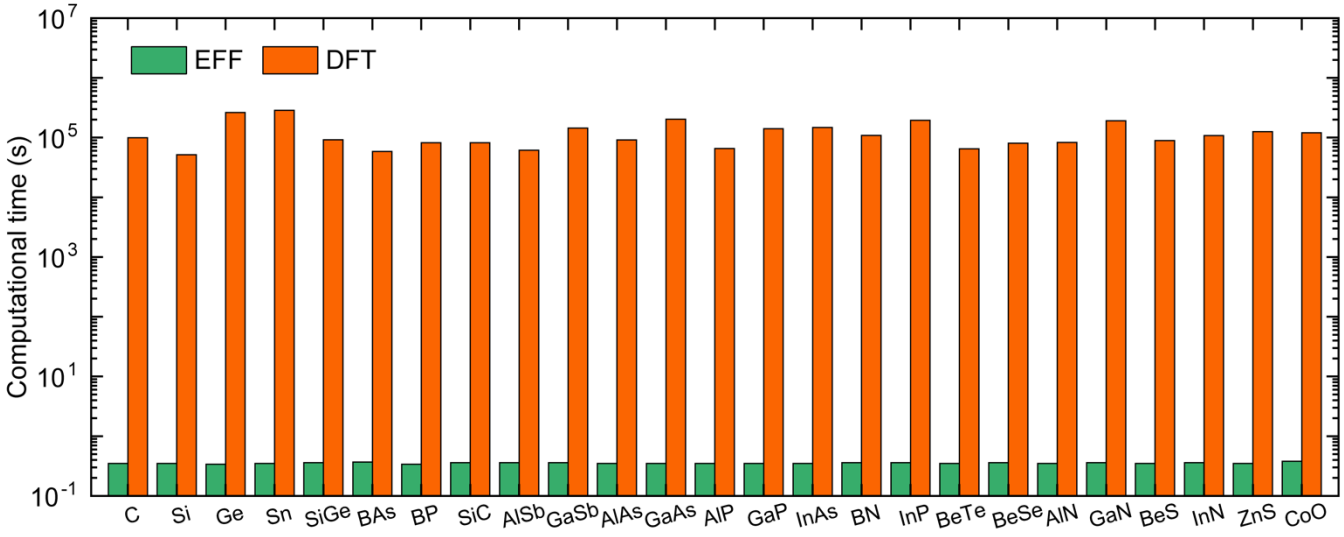

Figure S2. Computational time for elastic constants of 25 crystals in the training data set based on the EFF and DFT calculations.

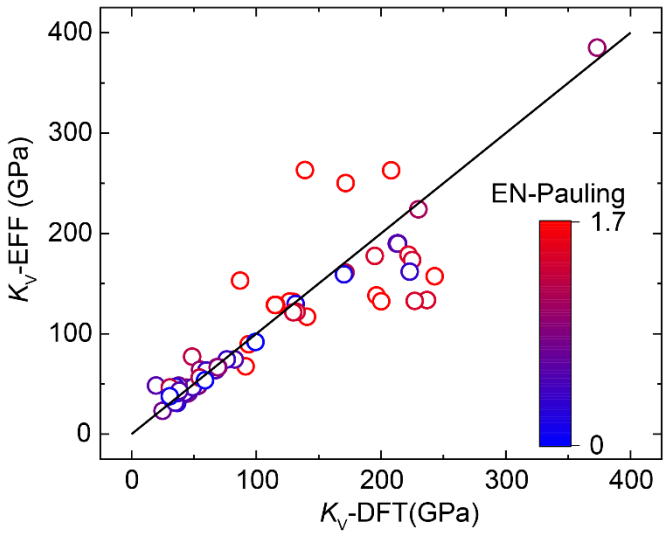

Figure S3. Predicted bulk moduli of 87 binary crystals from Material Project based on the EFF as compared with those from first-principles calculations. The crystals with Pauling electronegativity difference (EN-Pauling) between the two atoms larger than 1.7 are labeled with red color.

Table S1. Database statistics.

Database	Crystals	Elastic constants	Ref
Cambridge Structural Database, CSD	1,101,469	0	7
Open Quantum Materials Database, OQMD	815,654	0	8
Crystallography Open Database, COD	468,173	0	9
Inorganic Crystal Structure Database, ICSD	232,012	0	10
Materials Project, MP	131,613	13,172	11

Table S2. Diamond force field parameters and calculated bulk and shear moduli compared with well-known force field parameters in literature.[12-15]

Force field	k_b (eV/Å^2)	k_θ (eV)	K_V (GPa)	G_V (GPa)
DFT			431.8	519.8
EFF	14.448	4.765	432.7	518.3
UFF[12, 13]	15.168	9.289	463.4	546.0
CVFF[14]	13.994	2.021	424.2	286.4
PCFF[15]	12.995	1.714	382.9	262.8

Table S3. Parameters related to calculations of bulk and shear moduli for 25 typical unary and binary tetrahedral crystals.

Crystals	MP-ID	d (Å)	K_V (GPa)	G_V (GPa)	k_b-DFT (eV/Å^2)	k_θ-DFT (eV)	f_b	f_a	K_V-EFF (GPa)	G_V-EFF (GPa)
C	mp-66	1.547	431.8	519.8	14.448	4.765	0.000	0.000	432.7	518.3
Si	mp-149	2.368	89.0	64.1	4.555	1.740	0.000	0.000	80.0	63.4
Ge	mp-32	2.494	59.9	45.6	3.230	1.470	0.000	0.000	65.8	48.3
Sn	mp-117	2.880	35.9	20.1	0.000	0.915	0.000	0.000	37.5	18.7
SiGe	mp-978534	2.423	74.3	57.4	3.891	1.750	0.021	0.042	73.2	55.7
BAs	mp-10044	2.086	131.8	127.0	5.945	2.840	0.108	0.216	129.6	117.7
BP	mp-1479	1.969	161.9	164.9	6.891	3.243	0.143	0.285	159.3	149.1
SiC	mp-8062	1.896	212.0	195.7	8.693	3.430	0.206	0.413	189.9	185.0
AlSb	mp-2624	2.699	49.5	30.0	2.887	1.530	0.214	0.427	46.7	24.9
GaSb	mp-1156	2.692	44.9	29.2	2.611	1.510	0.214	0.427	47.0	25.1
AlAs	mp-2172	2.483	67.2	41.6	3.607	1.690	0.280	0.561	63.8	39.5
GaAs	mp-2534	2.490	60.1	42.1	3.235	1.784	0.280	0.561	63.3	39.2
AlP	mp-1550	2.384	82.8	49.4	4.268	1.760	0.312	0.625	74.3	48.4
GaP	mp-2490	2.384	76.4	53.5	3.939	2.003	0.312	0.625	74.3	48.4
InAs	mp-20305	2.680	48.5	26.0	2.808	1.450	0.341	0.682	47.3	23.3
BN	mp-1639	1.570	372.9	389.0	12.659	4.320	0.354	0.707	385.8	383.2
InP	mp-20351	2.579	59.7	33.3	3.327	1.662	0.372	0.743	54.7	29.0
BeTe	mp-252	2.455	56.5	41.5	2.998	2.129	0.413	0.826	60.0	26.4
BeSe	mp-1541	2.245	75.0	55.1	3.640	2.070	0.472	0.944	83.6	42.2
AlN	mp-1700	1.906	194.2	134.6	8.002	2.650	0.500	1.000	177.2	129.7
GaN	mp-830	1.970	170.2	112.6	7.250	2.410	0.500	1.000	160.5	117.5
BeS	mp-422	2.111	93.0	68.9	4.243	2.140	0.507	1.014	104.4	55.6
InN	mp-22205	2.186	121.4	53.9	5.740	1.560	0.549	1.097	109.0	68.8
ZnS	mp-10695	2.359	69.4	35.7	3.537	1.680	0.581	1.163	66.7	24.8
CoO	mp-19128	1.848	163.5	57.1	6.429	0.932	0.690	1.379	169.6	92.7

Table S4. Parameters related to calculations of bulk and shear moduli for 13 unary crystals.

Crystals	MP-ID	d (Å)	K_V-DFT (GPa)	G_V-DFT (GPa)	f_b	f_a	K_V-EFF (GPa)	G_V-EFF (GPa)
Sn	mp-949028	2.872	31.7	17.8	0	0	33.0	16.3
Ge	mp-128	2.528	52.3	39.4	0	0	59.4	45.3
Ge	mp-1007760	2.489	59.2	46.7	0	0	66.2	48.4
Si	mp-971662	2.375	76.3	45.2	0	0	69.4	55.7
Si	mp-971661	2.371	79.3	47.0	0	0	72.2	55.7
Si	mp-571520	2.383	80.6	62.5	0	0	75.0	60.7
Si	mp-999200	2.373	82.1	47.7	0	0	75.2	57.6
Si	mp-168	2.381	83.3	63.8	0	0	83.5	68.2
Si	mp-165	2.368	89.0	63.0	0	0	80.1	63.3
C	mp-47	1.549	435.4	529.1	0	0	431.7	519.5
C	mp-616440	1.548	435.6	522.7	0	0	432.6	518.6
C	mp-569567	1.548	435.6	522.5	0	0	432.0	518.0
C	mp-611426	1.548	435.8	525.1	0	0	432.3	518.9

Table S5. Parameters related to calculations of bulk and shear moduli for 63 binary tetrahedral crystals.

Crystals	MP-ID	d (Å)	K_V-DFT (GPa)	G_V-DFT (GPa)	f_b	f_a	K_V-EFF (GPa)	G_V-EFF (GPa)
CdSe	mp-1070	2.690	44.4	15.3	0.509	1.019	40.5	9.2
CdSe	mp-2691	2.690	45.0	16.8	0.509	1.019	40.5	9.5
HgSe	mp-820	2.717	41.3	15.2	0.509	1.019	39.3	9.2
HgS	mp-1123	2.601	49.3	17.6	0.509	1.019	46.6	13.1
CdS	mp-2469	2.572	53.3	19.4	0.509	1.019	48.1	13.6
CdS	mp-672	2.573	53.7	17.8	0.509	1.019	48.1	13.2
ZnTe	mp-2176	2.678	46.0	24.0	0.463	0.925	41.2	10.0
ZnTe	mp-8884	2.680	42.8	22.1	0.463	0.925	41.2	9.8
MgSe	mp-13031	2.598	44.0	17.4	0.488	0.976	46.4	12.9
MgS	mp-13032	2.467	54.7	22.0	0.488	0.976	56.2	18.2
ZnSe	mp-1190	2.486	58.7	29.2	0.463	0.925	54.8	18.2
ZnSe	mp-380	2.488	55.7	26.8	0.463	0.925	54.7	17.7
AlAs	mp-8881	2.483	67.7	40.0	0.271	0.543	63.8	39.2
AlN	mp-661	1.905	195.0	122.0	0.271	0.543	177.5	129.5
AlP	mp-8880	2.384	82.8	47.1	0.271	0.543	74.3	48.1
AlSb	mp-1018100	2.699	49.1	28.9	0.271	0.543	46.7	24.6
BAs	mp-984718	2.086	131.6	127.7	0.099	0.197	129.6	117.9
BN	mp-2653	1.571	373.2	386.7	0.099	0.197	385.2	383.5
BP	mp-1008559	1.969	170.3	160.0	0.099	0.197	159.2	149.2
GaAs	mp-8883	2.490	60.0	40.8	0.271	0.543	63.3	38.9
GaN	mp-804	1.968	171.6	106.7	0.271	0.543	160.9	117.3
GaP	mp-8882	2.384	76.4	52.3	0.271	0.543	74.4	48.1
InP	mp-966800	2.582	57.8	31.7	0.332	0.665	54.5	28.5
SiC	mp-7140	1.896	212.7	188.0	0.097	0.195	189.9	185.4
SiC	mp-568619	1.896	213.1	191.5	0.097	0.195	189.9	185.1
SiC	mp-9947	1.896	213.1	189.3	0.097	0.195	189.9	185.1
SiC	mp-568656	1.896	213.1	189.1	0.097	0.195	190.0	185.2
SiC	mp-568735	1.896	213.1	189.1	0.097	0.195	190.0	185.3
SiC	mp-7631	1.896	213.2	188.9	0.097	0.195	189.9	185.1
SiC	mp-568696	1.896	213.2	189.3	0.097	0.195	190.0	185.1
SiC	mp-570690	1.897	213.3	189.2	0.097	0.195	189.8	185.0
SiC	mp-582034	1.896	213.3	189.4	0.097	0.195	190.0	185.1
SiC	mp-570641	1.897	213.4	189.7	0.097	0.195	189.8	184.9
SiC	mp-11714	1.896	213.4	189.1	0.097	0.195	190.0	185.2

SiC	mp-570791	1.896	213.6	188.9	0.097	0.195	189.9	185.2
SiC	mp-570985	1.896	213.6	189.3	0.097	0.195	190.0	185.2
SiC	mp-567551	1.896	213.6	189.3	0.097	0.195	190.1	185.3
SiC	mp-567505	1.897	213.7	189.4	0.097	0.195	189.8	185.0
SiSn	mp-1009813	2.628	59.0	39.0	0.097	0.195	53.6	35.0
ZnS	mp-560588	2.361	68.4	33.1	0.463	0.925	66.5	24.2
ZnS	mp-554405	2.361	69.1	33.5	0.463	0.925	66.6	24.2
ZnS	mp-555763	2.360	69.2	33.3	0.463	0.925	66.6	24.3
ZnS	mp-555280	2.361	69.4	33.7	0.463	0.925	66.5	24.2
ZnS	mp-9946	2.361	69.4	33.9	0.463	0.925	66.5	24.2
ZnS	mp-10281	2.361	69.6	33.5	0.463	0.925	66.5	24.2
ZnS	mp-13456	2.361	69.6	33.7	0.463	0.925	66.5	24.2
ZnS	mp-561258	2.361	69.6	34.3	0.463	0.925	66.5	24.2
TlAs	mp-1007770	2.754	38.3	20.0	0.341	0.683	43.2	20.4
SnSb	mp-16365	2.996	30.7	20.2	0.185	0.370	37.6	26.3
MnTe	mp-1009222	2.769	19.7	16.0	0.257	0.513	48.4	32.8
MgTe	mp-1039	2.821	34.4	12.5	0.488	0.976	34.1	6.0
MgTe	mp-13033	2.820	32.7	13.6	0.488	0.976	34.1	6.2
MgSe	mp-1018040	2.597	30.7	20.6	0.488	0.976	46.4	12.6
InSb	mp-20012	2.872	35.0	20.4	0.332	0.665	36.1	14.2
HgTe	mp-2730	2.884	36.7	13.6	0.509	1.019	30.9	4.0
GaSb	mp-1018059	2.691	35.4	33.7	0.271	0.543	47.1	24.8
CuI	mp-673245	2.628	37.9	16.1	0.438	0.876	48.2	19.4
CdTe	mp-406	2.870	35.7	14.8	0.509	1.019	31.4	4.1
CdTe	mp-12779	2.872	35.1	13.5	0.509	1.019	31.3	4.0
AlBi	mp-1018132	2.792	37.0	22.8	0.271	0.543	40.8	19.5
AgI	mp-22894	2.875	24.9	6.1	0.726	1.453	23.1	19.2
CuCl	mp-22914	2.340	48.7	11.8	0.438	0.876	77.2	36.2
MnSe	mp-2293	2.575	55.0	15.0	0.257	0.513	64.2	46.4

Table S6. Bulk and shear moduli of 34 ternary tetrahedral crystals calculated by DFT and EFF.

Crystals	MP-ID	K_V-DFT (GPa)	K_V-EFF (GPa)	G_V-DFT (GPa)	G_V-EFF (GPa)
$BeGeP_2$	mp-1013527	71.8	87.6	66.5	59.5
$BeGeAs_2$	mp-1009088	63.7	74.2	53.4	47.9
$BeSiAs_2$	mp-1009087	73.6	79.0	58.3	52.2
$CuBS_2$	mp-12954	114.1	121.0	66.3	85.6
$AlCuS_2$	mp-4979	66.6	82.8	40.9	46.6
$ZnSiP_2$	mp-4763	84.6	77.7	55.9	45.9
$ZnGeP_2$	mp-4524	75.0	72.1	51.2	41.3
$ZnSnP_2$	mp-4175	63.8	60.9	40.9	31.4
$AlCuSe_2$	mp-8016	62.9	67.0	30.3	35.9
$GaCuSe_2$	mp-4840	59.7	65.7	30.4	35.2
$ZnSiAs_2$	mp-3595	66.1	65.2	44.3	35.8
$ZnGeAs_2$	mp-4008	60.6	60.8	38.9	32.2
$ZnSnAs_2$	mp-5190	52.4	52.1	32.1	24.5
$InCuS_2$	mp-22736	63.7	68.2	27.8	35.0
$MgSiP_2$	mp-2961	73.0	70.3	37.8	39.5
$MgSiAs_2$	mp-1016197	61.6	59.7	30.9	30.8
$InCuSe_2$	mp-22811	53.0	56.0	23.2	27.0
$AlCuTe_2$	mp-8017	51.6	49.7	25.9	23.4
$ZnSnSb_2$	mp-4756	40.4	39.3	24.3	13.5
$GaCuTe_2$	mp-3839	47.7	49.4	26.0	23.2
$TlCuSe_2$	mp-14090	46.8	53.1	19.5	25.2
$BeSiN_2$	mp-15704	231.3	229.7	186.2	180.1
$TlCuS_2$	mp-14089	56.7	63.8	24.6	32.3
$ZnCdTe_2$	mp-971837	37.8	35.9	19.3	6.5
$BeCN_2$	mp-15703	315.8	356.4	303.5	331.3
$MgSnP_2$	mp-1009083	57.0	55.0	28.4	26.3
$MgGeP_2$	mp-34903	64.9	65.0	34.1	35.2
$CuBSe_2$	mp-983565	76.8	95.7	52.1	65.3
$MgGeAs_2$	mp-1016200	52.3	55.3	27.2	27.4
$ZnCdSe_2$	mp-1017534	50.8	47.1	19.9	13.3

$AlGaN_2$	mp-1008556	184.3	168.8	122.6	123.7
$FeCuS_2$	mp-640073	52.7	94.8	19.2	66.6
$FeCuS_2$	mp-3497	56.7	95.3	20.6	66.2
$CrCdTe_2$	mp-1018083	40.2	40.4	16.5	16.4

Table S7. Mean error (ME), mean absolute error (MAE), mean relative error (MRE), and mean absolute relative error (MARE) of bulk and shear moduli for 110 covalent crystals (including 13 unary crystals, 63 binary crystals, and 34 ternary crystals) predicted by the EFF with respect to first-principles calculations.

	K_V-EFF	G_V-EFF
ME (GPa)	-1.79	-1.16
MAE (GPa)	8.85	7.58
MRE (%)	2.57	0.54
MARE (%)	11.27	28.28

Table S8. Mean error (ME), mean absolute error (MAE), mean relative error (MRE), and mean absolute relative error (MARE) of bulk moduli and shear moduli for 88 covalent crystals (including 25 fitting covalent crystals and 63 binary crystals) predicted by EFF and UFF[12, 13] with respect to first-principles calculations.

	K_V-EFF	K_V-UFF	G_V-EFF	G_V-UFF
ME (GPa)	-4.48	63.98	-3.37	53.78
MAE (GPa)	8.97	63.98	7.30	53.78
MRE (%)	0.01	65.62	-5.71	88.93
MARE (%)	10.55	65.62	26.29	88.93

Table S9. 25 covalent crystals with a bulk modulus over 350 GPa predicted by EFF and verified by first-principles calculations.

MP/OQMD ID	Crystals	K_V-EFF (GPa)	K_V-DFT (GPa)	Energy above hull (eV/atom)
mp-1078845	C	417.3	413.9	0.27
mp-1080826	C	407.5	402.0	0.30
mp-1190171	C	407.0	401.1	0.29
oqmd-637353	C	412.2	405.3	0.32
mp-47	C	431.7	432.7	0.16
mp-569517	C	432.6	432.6	0.14
mp-569567	C	432.0	432.6	0.14
mp-611426	C	432.3	432.7	0.15
mp-611448	C	432.5	432.6	0.14
mp-616440	C	432.6	432.5	0.14
mp-66	C	432.7	431.8	0.14
oqmd-603140	C	427.9	385.3	0.83
mp-13151	BN	365.9	351.1	0.18
mp-1639	BN	385.8	372.9	0.08
mp-2653	BN	385.2	373.2	0.09
mp-1095030	BC_7	395.1	389.8	0.28
mp-1079046	BC_7	394.7	390.7	0.24
mp-1078935	BC_7	394.3	392.9	0.21
mp-1079661	BC_7	394.0	393.5	0.24
mp-1080030	BC_7	394.3	393.3	0.24
mp-1077125	BC_5	382.4	379.9	0.24
mp-1077743	BC_5	382.2	377.4	0.26
mp-1018649	BC_5	382.0	378.2	0.27
oqmd-16166	BC_2N	409.5	377.9	0.53
oqmd-16167	BC_2N	409.9	377.6	0.53

REFERENCES

(1) Kresse, G.; Furthmuller, J. Efficient Iterative Schemes for *ab* Initio Total-Energy Calculations Using a Plane-Wave Basis Set. *Phys. Rev. B* **1996**, *54* (16), 11169-11186.

(2) Perdew, J. P.; Burke, K.; Ernzerhof, M. Generalized Gradient Approximation Made Simple. *Phys. Rev. Lett.* **1996**, *77* (18), 3865-3868.

(3) Monkhorst, H. J.; Pack, J. D. Special Points for Brillouin-Zone Integrations. *Phys. Rev. B* **1976**, *13* (12), 5188-5192.

(4) Voigt, W. *Lehrbuch Der Kristallphysik*; Teubner, 1928.

(5) Li, K.; Wang, X.; Xue, D. Electronegativities of Elements in Covalent Crystals. *J. Phys. Chem. A* **2008**, *112* (34), 7894-7897.

(6) Thompson, A. P.; Aktulga, H. M.; Berger, R.; Bolintineanu, D. S.; Brown, W. M.; Crozier, P. S.; in't Veld, P. J.; Kohlmeyer, A.; Moore, S. G.; Nguyen, T. D.; et al. Lammps - A Flexible Simulation Tool for Particle-Based Materials Modeling at the Atomic, Meso, and Continuum Scales. *Comput. Phys. Commun.* **2022**, *271*, 108171.

(7) Groom, C. R.; Bruno, I. J.; Lightfoot, M. P.; Ward, S. C. The Cambridge Structural Database. *Acta. Crystallogr. B. Struct. Sci. Cryst.* **2016**, *72*, 171-179.

(8) Saal, J. E.; Kirklin, S.; Aykol, M.; Meredig, B.; Wolverton, C. Materials Design and Discovery with High-Throughput Density Functional Theory: The Open Quantum Materials Database (OQMD). *J. Met. Mater. Miner.* **2013**, *65* (11), 1501-1509.

(9) Grazulis, S.; Chateigner, D.; Downs, R. T.; Yokochi, A. F.; Quiros, M.; Lutterotti, L.; Manakova, E.; Butkus, J.; Moeck, P.; Le Bail, A. Crystallography Open Database - An Open-Access Collection of Crystal Structures. *J. Appl. Crystallogr.* **2009**, *42* (4), 726-729.

(10) Zagorac, D.; Müller, H.; Ruehl, S.; Zagorac, J.; Rehme, S. Recent Developments in the Inorganic Crystal Structure Database: Theoretical Crystal Structure Data and Related Features. *J. Appl. Crystallogr.* **2019**, *52* (Pt 5), 918-925.

(11) Jain, A.; Ong, S. P.; Hautier, G.; Chen, W.; Richards, W. D.; Dacek, S.; Cholia, S.; Gunter, D.; Skinner, D.; Ceder, G.; et al. Commentary: The Materials Project: A Materials Genome Approach to Accelerating Materials Innovation. *APL Mater.* **2013**, *1* (1), 011002.

(12) Rappe, A. K.; Casewit, C. J.; Colwell, K. S.; Goddard, W. A.; Skiff, W. M. UFF, A Full Periodic Table Force Field for Molecular Mechanics and Molecular Dynamics Simulations. *J. Am. Chem. Soc.* **2002**, *114* (25), 10024-10035.

(13) Boyd, P. G.; Moosavi, S. M.; Witman, M.; Smit, B. Force-Field Prediction of Materials Properties in Metal-Organic Frameworks. *J. Phys. Chem. Lett.* **2017**, *8* (2), 357-363.

(14) Hagler, A. T.; Lifson, S.; Dauber, P. Consistent Force Field Studies of Intermolecular Forces in Hydrogen-Bonded Crystals. 2. A Benchmark for the Objective Comparison of Alternative Force Fields. *J. Am. Chem. Soc.* **2002**, *101* (18), 5122-5130.

(15) Sun, H.; Mumby, S. J.; Maple, J. R.; Hagler, A. T. An *ab* Initio CFF93 All-Atom Force Field for Polycarbonates. *J. Am. Chem. Soc.* **2002**, *116* (7), 2978-2987.